SYNTHESIS REPORT

FOR PUBLICATION

CONTRACT N° : BRE2-0453

PROJECT N° : ~~5442~~ BE- 5542

TITLE : PLASMA POLYMERISED COATINGS AND INTERPHASES FOR IMPROVED PERFORMANCE CARBON FIBRE COMPOSITES (PLASMA CFRP)

PROJECT COORDINATOR :

UNIVERSITY OF SHEFFIELD (UK)

PARTNERS :

KATHOLIEKE UNIVERSITEIT LEUVEN (B)
INSTITUT FUR KUNSTSTOFFVERARBEITUNG (D)
LULEA UNIVERSITY (S)
ESCUELA TECNICA SUPERIOR DE INGENIEROS INDUSTRIALS, SEVILLE (ES}

STARTING DATE : 1/7/93 DURATION : 36 MONTHS

PROJECT FUNDED BY THE EUROPEAN COMMUNITY UNDER THE BRITE/EURAM PROGRAMME

DATE : 14/6/96

2. TITLE AND AUTHORS NAMES AND ADDRESSES:

PLASMA POLYMERISED COATINGS AND INTERPHASES FOR IMPROVED PERFORMANCE CARBON FIBRE COMPOSITES

M. R. Alexander, R. D. Short and F. R. Jones
Laboratory for Surface and Interface Analysis, Department of Engineering Materials, University of Sheffield, Sir Robert Hadfield Building, Mappin Street, Sheffield, S1 3JD, United Kingdom.

M. Stollenwerk, G. Mathar, J. Zabold and W. Michaeli.
Institut Für Kunststoffverarbeitung (IKV), Pontstrasse 49, RWTH Aachen, D-52056 Aachen, Germany.

J. Varna, R Joffe and L. Berglund
Department of Materials and Production Engineering, Luleå University of Technology, S-95 187, Luleå, Sweden.

Wu Wei, E. Jacobs, M. Desaeger and I. Verpoest
Department of Metallurgy and Materials Engineering. (MTM), Katholieke Universiteit Leuven, de Croylaan 2, B -3001 Leuven, Belgium.

F. paris
Escuela Tecnica Superior de Ingenieros Industriales, Grupo de Elasticidad y resistencia de Materials, Avda Reina Mercedes s/n, 41012 Servilla, Spain.

3. ABSTRACT:

Plasma deposits on flat substrates have been characterised using nanoindentation and chemical surface analysis. The chemistry was found to change from organic to inorganic with the addition of oxygen to the plasma. A corresponding increase in the modulus of 3-5.5 GPa was found from nanoindentation tests. Equivalent coatings were deposited onto untreated, unsized carbon fibres. These fibres were then impregnated with resin to form single filament fragmentation test (SFFT) specimens, and in bundles to form composite rods. An adhesion promoting oxygen pre-treatment was applied and optimised using the SFFT in combination with SEM fractography. The influence of a high modulus coating upon micro and macro-mechanical properties was measured using SFFT, tensile and torsional testing of the composite rods. Using models of these 3-phase systems, the properties of the coating within the composite were found to agree with estimates predicted from the coating chemistry, via its correlation with the values determined separately by nanoindentation. Estimates of the fracture toughness (G_C) of the interface between fibre and matrix in a 2 phase composite has been made. The models are being applied to the estimation of the fracture toughness of an $HMDSO/0_2$ plasma interphase.

4. INTRODUCTION:

It is now being recognised[1-4] that the sizing resins used to protect fibres from damage need to be designed for compatibility with the matrix resin to form a reproducible interphase region rather than the uncertainty which exists with current practice. For example Reifsnider[5] and co-workers has modelled the effect of a polyvinyl pyrrolidone coating on the durability of a composite under fatigue loading. With the development of high performance resins it is necessary to provide an environmentally friendly coating system, which can be easily switched from say e.g. an epoxy resin compatible size to a bismaleimide, or thermoplastic compatible size. The interracial and interphase properties would always be optimum. Ideally the technology should replace both the surface treatment (electrolytic) and aqueous emulsion sizing stage. Plasma polymerisation represents an ideal technology which can be environmentally friendly and facilitate easy changes in deposit composition and structure. Potentially the activated nature of the process provides for the replacement of the current oxidation and sizing stages. The role of the interphase has also been shown to influence the nature of the stress transfer between the fibre and matrix and the growth of interracial cracks. A major objective therefore is to identify the fundamental requirements for the mechanical properties of the distinct interphase.

Using a computer lattice model, Termonia[6] showed that a fibre coating layer decreased the stress concentration and improved the load carrying capabilities of a broken fibre. He suggested that the optimum fibre coating must have a modulus 1-2 times that of the matrix and a thickness of about 100 nm. However the model assumed the presence of a low modulus 'mesophase' between the coating and the matrix. There has been no reported systematic study of the role of an interphase in fibre composites. This study uses plasma polymerisation to obtain a coating on carbon fibres of this thickness and modulus combination to investigate the effect of an interphase.

Plasma polymerisation is a vacuum coating technology. The chosen monomer is allowed to flow into a reaction chamber. Here, it is partially broken down by the application of a strong oscillating electric field to give reactive components, including ions, electrons and radicals. Recombination of these species at a substrate surface produces a solid plasma deposit.

In this project, plasmas were sustained using microwaves to produce deposits with mechanical properties and chemistries ranging from those of inorganic to polymeric materials. Carbon fibres coated with a modulus approximately 2 times greater that the matrix were embedded in epoxy resin as single filaments, and bundles to provide model composites with a distinct interphase in the modelling of this 3-phase system, has enables the properties of the coating or interphase within the composite to be estimated. These were found to agree with estimates obtained from the structural/nanoindentation correlation. Interracial damage occurring during the fragmentation of a single embedded filament has been examined using electron microscopy.

5. TECHNICAL DESCRIPTION:

5.1 Plasma deposition

Plasma polymerisation has been used to provide a carbon fibre surface with a coating which will form a distinct interphase when embedded in resin. The equipment used is illustrated in Fig. 1. The typical process parameters employed were a power of 200 W with a monomer flow rate of 20 sccm[7]. Initially a continuous fibre coating device was used, but it was found to be deficient in applying a homogeneous and uniform coating. A batch process was used to overcome problems associated with inadequate spreading of the tow and the resultant poor coating uniformity. It is envisaged that on-line processing with sophisticated fibre spreading would allow this problem to be overcome.

5.2 Fibres and resin

The carbon fibres used in this programme were supplied in an untreated-unsized form (HTA-5000) by Tenax Fibers Gmbh. This is a high-performance carbon fibre manufactured from a polyacrylonitrile (PAN) precursor, with high-strength and standard modulus similar to the more familiar Toray T300. The 7 μm fibres are supplied as 12,000 filament tows, with reported values of the tensile modulus, strength and failure strain of 238 GPa, 3.9 GPa and 1.4% respectively.

The resin matrix was a novolac epoxy (LY5052) containing 1, 4-butanediol diglycidylether which is cured by 38%wt of an aliphatic polyamine hardener (HY5052), supplied by Ciba Geigy. The cured resin(15 hrs 80°C) has an elastic modulus of 3.0 GPa, a tensile strength of 71 MPa and a failure strain of 6-8°/0. The shear yield strength of the resin, 41 MPa, was evaluated from the measured tensile yield strength using the von Mises relationship.

5.3 Nanoindentation

The nanoindentation technique is one that has been widely applied to metals and ceramics. its development for application to viscoelastic, polymeric materials is dealt within detail elsewhere. It is sufficient to note here that at coating thicknesses of less that 5 μm the substrate has an influence that provides misleading results. Also, care must be taken with the loading speed, standard 10 $nm\,s^{-1}$ (10-320 $nm\,s^{-1}$). Under these conditions the Young's modulus of the coatings may be determined.

5.4 Chemical Surface Analysis

All XPS analyses were carried out using a VG CLAM 2 electron analyser and Mg kα x-radiation. For the purpose of elemental quantification we have used sensitivity factors experimentally determined from a PDMS polymer

standard (Aldrich). The energy scale of the instrument was calibrated using a gold standard and verified with the separation of the C 1s and F 1s peaks from PTFE. Full details of the experimental conditions have been discussed elsewhere[7].

5.5 Micromechanical testing

The single fibre fragmentation test (SFFT) was used to assess the interfacial micromechanics. The full experimental details have been given elsewhere[8].

5.6 Composite Rod Fabrication

Composite rods were fabricated from fibre bundles containing 12,000 filaments using the method illustrated in Fig 2. This type of specimen was chosen because of the limited number of filaments that could be coated uniformly using the batch process. Tapered end-tabs were attached to the coupons to provide good load transfer from the grips during monotonic and torsional loading. Full details of the fabrication and testing of these model composite bars is given elsewhere[9].

6. RESULTS:

6.1 Relationship between Plasma Polymer Structure and Tensile Modulus

Plasma deposits have been formed from a selection of monomers (ethylene, butadiene and hexamethyldisiloxane-HMDSO) on a variety of substrates (polycarbonate, glass, graphite, aluminium, and carbon fibre). On the basis of deposition rate and ease of handling, HMDSO was selected as the monomer for this study. There also exists a considerable literature on this plasma system[10]. The deposition rate was typically 1 μm/min, and coatings of 0.1 and 0.5 μm were produced to investigate the effect of thickness. A typical coating is illustrated in the electron micrograph in Fig 3. The conditions chosen provided a poorly adhering coating to the carbon fibre, so on fracture of the fibre the coating debonds and can be clearly seen in the micrograph. The adhesion of the coating could be controlled by employing an oxygen plasma pre-treatment. This was found to be necessary because of the fibre, although untreated, was obtained by interrupting the commercial process. It is possible that a pre-treatment would not be necessary for an on-line water. The micrograph also shows the conformal nature of the coating process.

Nanoindentation Test of plasma deposits on polycarbonate substrates indicated that the addition of oxygen to the HMDSO monomer feed produce a harder coating. Deposits formed from HMDSO alone had a Young's Modulus of 2.6 GPa. The addition of oxygen to the plasma (20 seem HMDSO, 200 seem 0_2) increased the modulus to 5.5 GPa. The higher value provided the condition outlined by Termonia[6], discussed above, of $E_{coating} \approx 2E_{matrix}$, for the epoxy resin system (E_{matrix}= 2.7 GPa).

X-ray photoelectron Spectroscopy has been used to characterise the chemical structure of these thin films. This work is presented in more detail elsewhere*. It is sufficient to note that the position of the XPS Si2p peak is indicative of the chemical state of the silicon atoms in the deposits. The effect of oxygen addition to the plasma upon the Si2p binding energy is presented in Fig 4 along with the chemical structures of the silicon environments that are indicated. Equivalent changes to the elemental composition of the deposit are shown in Fig 5. This shows that the average chemical structure of the deposit changes from mainly polymeric to mainly inorganic on adding 0_2 to the plasma gases. It is apparent that the structure has been achieved of silica and can not b e obtained even by the further addition of oxygen to the plasma. The change in structural chemistry correlates with the increase in the Young's Modulus obtained from the nanoindentation test.

6.2 Micromechanics of Composites with a distinct interphase

The **single filament fragmentation test (SFFT) was** used to determine the shear strength of the interface of uncoated fibres. The detailed description of the technique and the theory may be found elsewhere [1]$. The test results are presented in the form of number of fibre fragments formed as a result of tensile extension of the coupon. Because no theory satisfactorily converts this observation to an interracial shear strength, this is not reported. This data provides a qualitative measure of the qualify of the. interface, the larger the number of fragments the more efficient the stress

transfer by the interface/interphase. Examination of the tested sample in polarised light also provides valuable information on the nature of the interface/interphase failure mechanisms. Both these are presented in Table 1. It is apparent from these data that the introduction of a plasma polymer coating substantially reduced the number of fragments, from 20 to 10 and had effected the quality of the interphase. Thus the interphase was accompanied by an interface of lower shear strength. A number of plasma pre-treatments (N_2, 0_2 and Ar) were carried out to improve this, the results are included in Table1 . As can be seen, all of these samples, except for those with an oxygen pre-treatment had relatively poor adhesion, as indicated by a low fibre fragment number in comparison to the 'uncoated case'. This indicates that the weaker interface was that between the fibre and the plasma deposit. By chemically modifying the carbon fibre surface oxygen pre-treatment improving the interracial shear strength the fibre surface. We believe that the alternative hypothesis that the oxygen pre-treatment only removes hydrocarbon and other contamination from the fibre surface is unlikely because the Ar treatment would have had the same effect, and yet failed to improved the interracial bond. km-easing the power of the oxygen plasma pre-treatment to the maximum possible in this apparatus provided the highest degree of adhesion as indicated by a fragment number of 25. Additional information on the locus of interracial or interphase failure could also be obtained by examining the coupon in polarised light since the matrix resin is photoelasticf

A change in the nature of interracial failure was also observed using polarised light as the fragment number increased. Poor results on coated fibres were characterised by a completely dark interface. As the oxygen pretreatment improved the fibre-coating interface, the debond was characterised by a bright zone. Bright interface zones were also observed for the uncoated fibres. In the case of uncoated fibres a bright debond indicates an interracial failure where stress transfer still exists. The dark region indicates that frictional stress transfer to the photoelastic matrix was absent. Therefore, a more complex mechanism had occurred in the interphase region.

Comparison with the SEM fi-autography suggested that failure at the fibre-coating interface is characterised by a dark failure zone. As the strength of this interface increases, the locus of the failure changes from the fibre- coating to the resin-coating interface. In this instance we believe the brightness is indicative of cracks located at the resin-coating interface, while the dark zone is indicative of fibre-coating interface failure, and possibly the crack path running within the interphase.

The schematic diagram in Fig 6 demonstrates that the interracial crack is initiated at the fibre-coating interface and then passes through the interphase before running principally along the coating-matrix interface. Finite element analysis of a well-bonded interphase (E=5.67 GPa) supports the initiation of interracial failure at the fibre-coating interface, because it was shown that shear stresses were higher here that at the coating-matrix interface[1]. The differences between the light and dark debond zones probably reflect the different friction coefficient between fibre and coating and coating and matrix.

A dark debond corresponds to a low fringe order and would imply a very low interracial stress transfer. This may arise either as a consequence of the structural

failure of the coating, or as a result of the low coefficient of friction between the adj scent surfaces. A bright interface, on the other hand is indicative of a high degree of frictional stress transfer and/or non-recoverable plastic deformation of the matrix. When bright and dark failure mechanisms are observed this is indicative of both processes occurring along one debond. This is illustrated schematically in figure 6.

SEM fractography of the SFFT samples confirmed the hypothesis that the weaker interface was that between the fibre and coating. The cross-sections illustrated in Fig 7 are taken from SFFT samples, they have been cut and then polished. Fig 7a is a coated sample that has not been tested. It is clear that the interphase is intact and the polishing in the sample "preparation does not introduce artificial damage. The failure of the fibre-coating interface is well illustrated in fig 7b a 200W pre-treated sample. Here the coating can clearly be seen to have separated from the fibre as a result of interracial debonding during the SFFT with a 600 W $.0_2$ pre-treatment the interracial crack path runs between the fibre-coating interface (Fig 7c), and the coating resin interface (Fig 7d), along the fibre. This suggests that good energy absorption properties may be attained with this pre-treatment/coating system.

Comparison with commercially surface treated fibres

In order that the performance of the interphase may be compared with that of commercially available carbon fibres, sized Tenax HTA with conventional surface treatment, a separate study was carried out in Sheffield. Slightly different results are consistently obtained and therefore the data in Table 2 may only be compared with itself and not the previous two tables (trends obtained in the two laboratories are consistent).

This data indicates that the commercially available surface treated fibres (sized) give a relatively high fragment number (34). It is apparent however that this was not as high as that obtained with a plasma polymer coated fibre (39). This suggests an improved stress transfer using the plasma deposit coated fibre. It is also interesting to note that matrix cracking was observed when the commercially sized fibre was used, whereas this was absent with the plasma coated sample. This is indicative of the deleterious effect of the size upon the properties of the cured resin around the fibre 12 Thus the plasma deposit coated fibre represents a considerable improvement upon commercially available fibres.

6.3 Mechanical Performance of Composites containing carbon fibres with a distinct interphase region

Composite rods have been fabricated from **fibre bundles** for testing under tensile and torsional loads. In this way the macromechanical properties of a fibre composite with defined interracial properties can be studied.

In the **tensile tests,** the longitudinal Young's modulus for the different specimens is effectively determined by the fibre properties, therefore it is more relevant to compare the failure strains or strengths. Values of failure strain and the type of failure are summarised in Table 3. A macroscopically brittle failure is called here a type 1

failure. Type 2 and type 3 failure modes are rather tough, wherein the case of type 3 very long interracial debonds have occurred prior to failure.

In the case of the poorly adhering interphase, the failure strain of the composite will be larger than that with perfect bonding between fibre and matrix. Indeed, the released energy, when a weak fibre breaks, will cause long fibre-matrix or fibre-coating interracial debonds. A long interracial debond reduces the stress transferred to the unbroken neighboring fibres and therefore inhibits the failure process. This phenomenon is observed for the specimen containing untreated, uncoated fibres, as well as for the untreated fibres with a 0.1 μm coating. If adhesion is good, the observed failure strain will depend on the toughness of the interphase. In the case of a strong and adhered interphase, when the fibre fails a crack will form in the interphase and continue to grow into the matrix leading to failure of neighboring fibres. In this case only a few fibre breaks are needed to cause composite failure. This process leads to a composite with a very low failure strain, as happened 600W pretreated fibres with no coating. If the interphase adhesion is less strong or if it has a high fracture toughness then cracks can occur in these interracial areas which do not lead to failure of the composite. In this way, a part of the energy, released at the fibre break, can also be absorbed, leading to a composite with a higher failure strain. The interracial debond will probably be shorter than in the case of poorly adhering interphase. The fracture toughness of the coating used in this project is of the same order of magnitude as the fibre-coating interracial fracture toughness, therefore, an existing crack can grow into the coating layer. The two extreme cases of failure, type 1 and type 3 are shown in Fig 8a and 8b respectively.

Torsion tests have been performed for as received fibres, uncoated pretreated fibres (600W), and 600 W pretreated fibres with both 0.1 and 0.5 μm thick coatings. Short cylindrical specimens are loaded in torsion (length= 5 **cm).** As the fibres are aligned in the **axial** direction of the specimen, damage development will not immediately lead to composite failure but only after substantial damage to the composite has occurred.

The analysis is therefore focused on the torsional stiffness results. The test results for the axial shear modulus of the composite $G_.$ are shown in Table 3, as well as values from model calculations. The dependency of the axial shear modulus towards the fibre coating (in a coated fibre composite) can be predicted, using a theoretical model for unidirectional laminates. Using the homogenisation method, a closed-form solution for the axial shear modulus of a composite ($G_{theor.}$) can be obtained as a fiction of the axial shear modulus of the carbon fibre and the shear modulus of the isotropic epoxy matrix. The expression is given by:

$$G_{theor.} = G_M*(I-II)/(I+II)$$

$$\text{with } I = (2\alpha+1)^2*(G_C+G_F)*(G_M+G_C)+(G_C-G_F)*(G_M-G_C)$$

$$H = [(2\alpha+1)^2*(G_C+G_F)*(G_M-G_C)+(G_C-G_F)*(G_M+G_C)]*V_f*(2\alpha+1)^2$$

$$\alpha = (r_C-r_F)/(2r_F)$$

where $G_{M,F,C}$ are the axial shear modulus of respectively matrix, fibre and coating, Vf is the fibre volume fraction and $r_{F,C}$ the fibre radius and the outer coating radius.

Using the following appropriate material data: G_F = 2.6 GPa,- E_M = 3.2 GPa, E_C = 5.5 GPaand V_F = 0.51.

the theoretical shear modulus of composites containing uncoated, 0.1 μm thick coated and 0.5pm thick coated fibres were calculated to be 3.17 GPa, 3.26 GPa and 3.67 GPa respectively. This is a good agreement between the experimental data shown in Table 4.

Transverse testing of single fibres and fibre bundles embedded in resin was performed in order to determine fracture toughness of the interface and to evaluate composite transverse strength. Micromechanical models for fracture toughness testing were developed in order to relate composite transverse properties to the properties of a fibre coating/interphase. This model also enables the coating stiffness to be determined from the transverse stiffness of the composite as can be seen from the graph in Fig 9.

A micromechanical model has been developed which relates the transverse properties of a composite to the properties of a distinct interphase. From the experimental values of the fibre, matrices, and composites the modulus of the coating can be estimated. Furthermore the growth of a debond along and around the circumference of an embedded fragment under transverse loading, has been modelled for both 2 and 3 phase systems using FEM and BEM stress analysis. In this way the fracture toughness of an interface or an interphase can be estimated from a transverse test on a singles embedded filament which has previously been fragmented under tension. Typical results of these calculations are given in Fig 10 where the theoretical strain energy release rate is shown to be independent of the fibre diameter. As expected the highest resistance to crack growth is provided by good interracial adhesion.

The stress required for the propagation of an interracial crack as monitored by the growth of an arc around the model fibre, under a transverse load is given in Fig 10. The BEM method is much better at predicting experimental values. By comparing the theoretical predictions for a given value of interfacial fracture toughness (G_C = 25 Jm^{-2}) with experimental observations the stress required for debond growth, a value of fracture toughens, can be obtained. The data are for a poorly bonded glass fibre-resin system (?). Of more relevance to the 3-phase system studied here is requirements of the coating on interracial fracture toughness. It is clear from Fig 11 that the interracial fracture toughness (strain energy release rate) is a function of the fracture surface area which is directly related to the diameter of the fibre. This failure at the coating-matrix interface is predicted to give the highest value of G_C. However, this model ignores the contribution of interphacial crack growth implicit in Fig 6d.

Improved analytical micromechanical models of the fragmentation of the single embedded filament has also been developed. The stress transferred to a single embedded coated fragment has been model led analytically. In Fig 13 the predictions

of the current analytical model (Fig 14) are compared to the FEM stress analysis. The analytical model is currently being improved to provide abetter description of the stress transfer process.

The stress redistribution within a fibre bundle when the fibres break has also been modelled. The effect of coating properties on the stress concentration factors has also been estimated. A model for the transverse cracking of an impregnated bundle under transverse loading has also been developed for the prediction of transverse strength and fracture toughness of a composite. These models are discussed elsewhere (?).

7. CONCLUSIONS:

A batch plasma deposition process for forming homogeneous coatings on carbon fibres with uniform thickness, in the range 0.1-0.5 pm, has been developed. By varying the ratio of HMDSO and O_2 in the plasma, a range of coatings with moduli, 2.6-5.5 GPa, as determined from nanoindentation tests on coatings on flat substrates, can be obtained. It is anticipated that more sophisticated on-line fibre handling equipment will allow this batch process to be adapted to the continuous coating of large quantities of fibres. When embedded into a matrix a distinct interphase region of controlled properties is obtained.

Single fibre fragmentation testing of the fibre/coating/matrix model composites has shown that for a HMDSO/O_2 coating (E=5.5 GPa), a strong interface between coating and fibre can be achieved using an oxygen plasma pretreatment. By adjusting the plasma parameters the path of interracial cracks can be changed from one interface through the coating interphase and to the other interface. In some case mixed mode failures were observed. The adhesion of the interphase has a strong influence on the tensile breaking strain of the composites. These tensile breaking strain results were also consistent with the micromechanical test data. Torsional testing of composite rods formed from impregnated bundles has allowed the determination of composite stiffness and the Young's and Shear Moduli of the interphase or coating. The modulus of the coating determined using this method agrees with values obtained from nanoindentation tests on flat plasma deposits.

Using the fragmentation test the performance of the coated fibre was determined to be superior to that of commercially available treated and sized fibres. Superior stress transfer through the interphase was attained whilst avoiding matrix cracking caused by dissolution of size into the resin matrix.

A methodology for the determination of the fracture toughness of the interphase and the coating-fibre and coating-matrix interfaces has been developed. These models may be used to simulate debonding in a three-phase composite and describe failure of an impregnated bundle. In this way the macro-properties of a unidirectional laminate can be inferred from the properties of an impregnated bundle.

8. ACKNOWLEDGEMENTS

The EC is acknowledged for funding this project entitled 'Plasma polymerised coatings and interphases for improved performance fibre composite' Proposal No 5542, contract number BRE2-0453. The help of the endorsers of this project is acknowledged; Daimler Benz, Tenax, Brouchier S. A. and Ciba Cigy.

9. REFERENCES

1. J. L. Thomason in Interfacial Phenomena in Composite Materials Ed F. R. Jones, ButterWorth, 1989.

2. G. Wachinger in Interfaces in Polymer, Ceramic and Metal Matrix Composites. Ed H. Ishida, Elsevier 19S8 pp 457-468.

3. L. Drzal and M Madhukar in Journal of Material Science, 1993. pp 28,569.

4. F. R. Jones in Key Engineering Materials 1996, 116-117, p. 41.

5. K. Reifsnider in Composites 1994,25, p. 461.

6. Y. Termonia, 'Fibre coating as a means to compensate for poor adhesion in fibre-reinforced materials'. J. Mater. Sci. 25 (1990) p. 103.

7. M. R. Alexander, R. D. Short, F. R. Jones, M. Stollenwerk, J. Zabold, and W. Michaeli "An XPS investigation into the chemical structure of deposits formed from hexamethyldisiloxane/oxygen plasmas", J. Mater.Sci.,31 pp 1879-1885 (1996).

8. W. Wu, E. Jacobs, L Verpoest, A. P. Kettle, F. R. Jones, M. R. Alexander, M. Stollenwerk, J. Zabold and W. Michaeli, 'Experimental evacuation of the interphase region for carbon fibre composites with plasma polymerised coatings', published in ECCM-7, Realising their commercial potential Vol. 2, Woodhead Publishing, Cambridge, UK. 1996, pp 154-158.

9. E. Jacobs and I. Verpoest in preparation.

10. "Plasma deposition, treatment, and etching of polymers", Edited by R. d'Agostino, Academic Press, 1990.

11. F. Chen, D. Tripathi and F. R. Jones, 'Determination of the interracial shear strehgth of glass fibre reinforced phenolic composites by a bimatrix fragmentation test', *Composites Sci. Tech.*, (1996) in press.

12. Drzal, L. T. and Madhukar, M., 'Fibre-matrix adhesion and its relationship to composite mechanical properties', *J. Mater. Sci.*, *28* (1993) pp. *569-610.*

11. L Verpoest and M. Desaeger, 'Interracial bond strength determination-fragmentation' in Handbook of polymer composites Ed. F. R. Jones Longman 1994, pp 235-238.

12. A. P. Kettle, W. Wu, M. Stollenwerk, R. D. Short, F. R. Jones, M. R. Alexander, 'Experimental evaluation of the interphase region for carbon fibre composites with plasma polymerised interphases' paper in preparation.

TABLES

fibre pretreatment	coating thickness	average fragment number	Debond under polarised light	Locus of failure
	uncoated	20 ± 3 (15)	bright debond	fibre-matrix
None	0.1 μm	10*1 (5)	dark interface	fibre-coating
"	0.5 μm	10 ± 2 (5)	dark interface	"
200W O* post-treatment only	0.1 μm	9 ± 2 (5)	dark interface	"
O_2 200 w	0.5 μm	17 ± 4 (7)	dark interface	"
0'2200 w	0.1 μm	20 ± 5 (9)	bright/dark interface	coating-matrix/fibre-coating
O_2 600 W	0.5 μm	**21** ± 6 (14)	**bright/dark interface**	coating-matrix/fibre-coating
O_2 600 W	**0.1 μm**	25 ± 7 (23)	**bright/dark interface**	coating-matrix/fibre-coating
$0_2$600 W	uncoated	41 ± 4 (20)	bright debond	fibre-matrix
$0_2$600 W + acrylic acid post-treatment	0.1 μm	37 ± 8 (9)	bright/dark interface	coating-matrix/ fibre-coating

Table 1 Effect of plasma pretreatment upon the SFFT of coated and uncoated carbon fibres. The figures in parentheses are the number of tests to obtain the mean.

fibre	coating thickness	average fragment number	Locus of failure
Untreated	uncoated	19 ± 3	fibre-matrix
Commercially treated-unsized	uncoated	30 ± 4	fibre-matrix
Commercially treated and sized	uncoated	34 ± 3	fibre-matrix with transverse matrix cracks
O_2 600 W pretreated HMDSO/O_2 coated	0.1 μm	39 ± 7	mixed interfacial mode

Table 2 Fragmentation test results performed at The University of Sheffield.

Oxygen Pretreatment		600W	-	200W	600W	600W
coating thickness/pm			0.1	0.1	0.1	0.5
ε_{mean} /%	1.14	0.83	1.16	1.07	1.00	0.89
Failure type	type 3	type 1	type 3	type 2	type 2	type 2

Table 3: Tensile failure strains for cylindrical composite specimen

	Torsion results for different composite specimen			
Oxygen pretreatment		600 W	600 W	600 W
Coating thickness /μm			0.1	0.5
G_{ave}/GPa	3.2±0.2	3.2 ±0.4	3.3±0.4	3.6 ±0.3
$G_{theor.}$	3.17	3.17	3.26	3.67

Table 4: A comparison of experimental and theoretical shear moduli for differing composite systems. Gave is the average of 6-7 specimens.

FIGURES

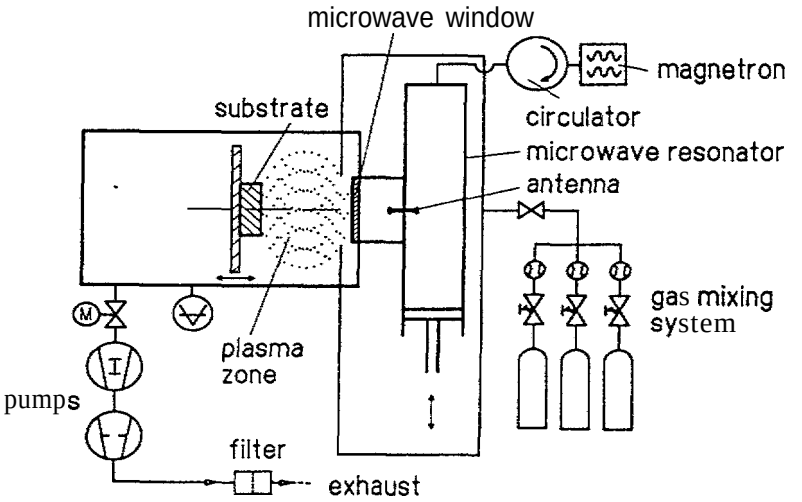

Figure 1 Schematic illustration of the plasma deposition apparatus

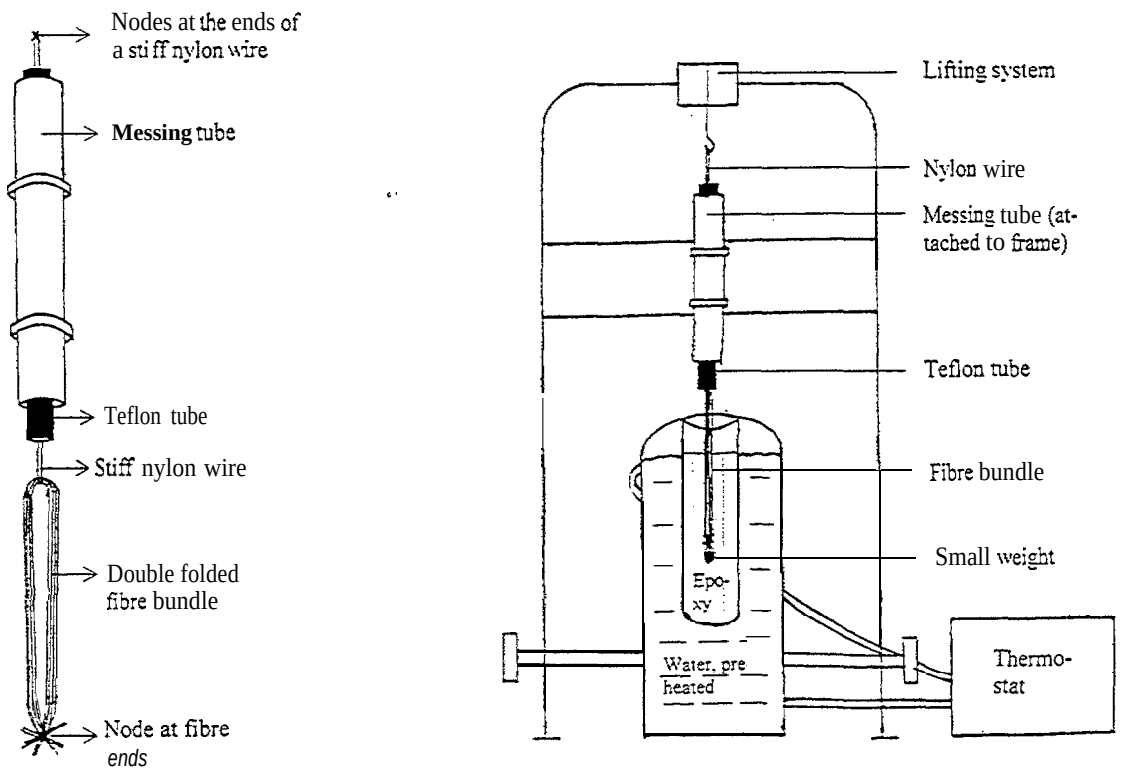

Figure 2 The fibre bundle impregnation method.

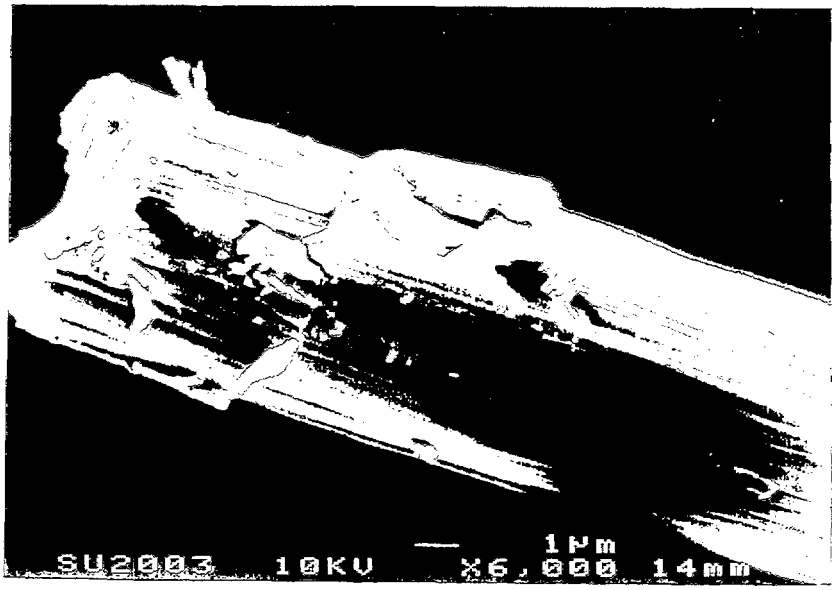

Figure 3 Electron micrograph of a plasma deposit on a carbon fibre.

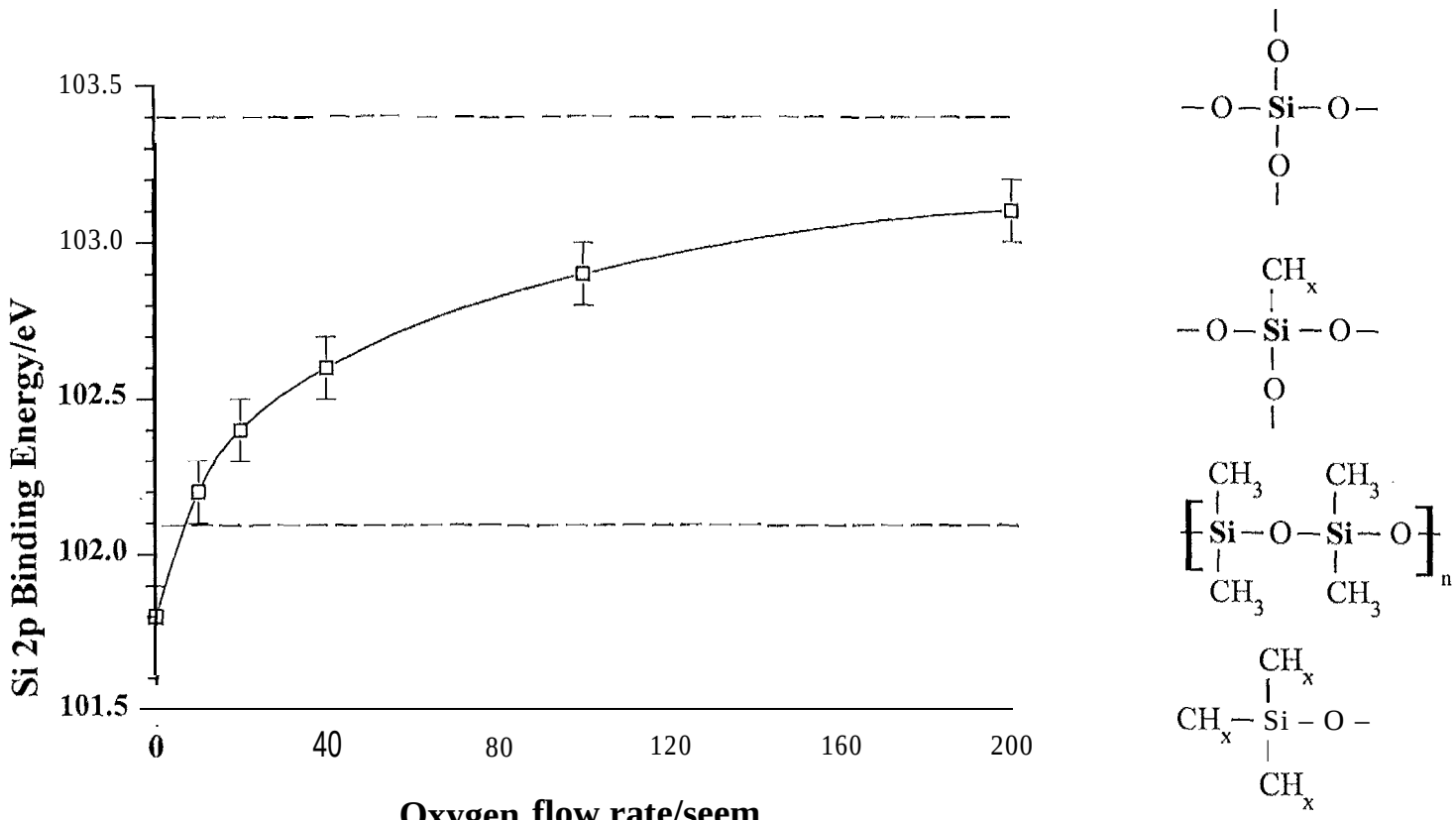

Figure 4 XPS Si2p peak binding energy from HMDSO/O_2 plasma deposits -P=50 pa, W=200 W, HMDSO flow=20 seem, film thickness=5 μm versus oxygen flow rate/seem. Alongside are silicon environments corresponding to these peak positions.

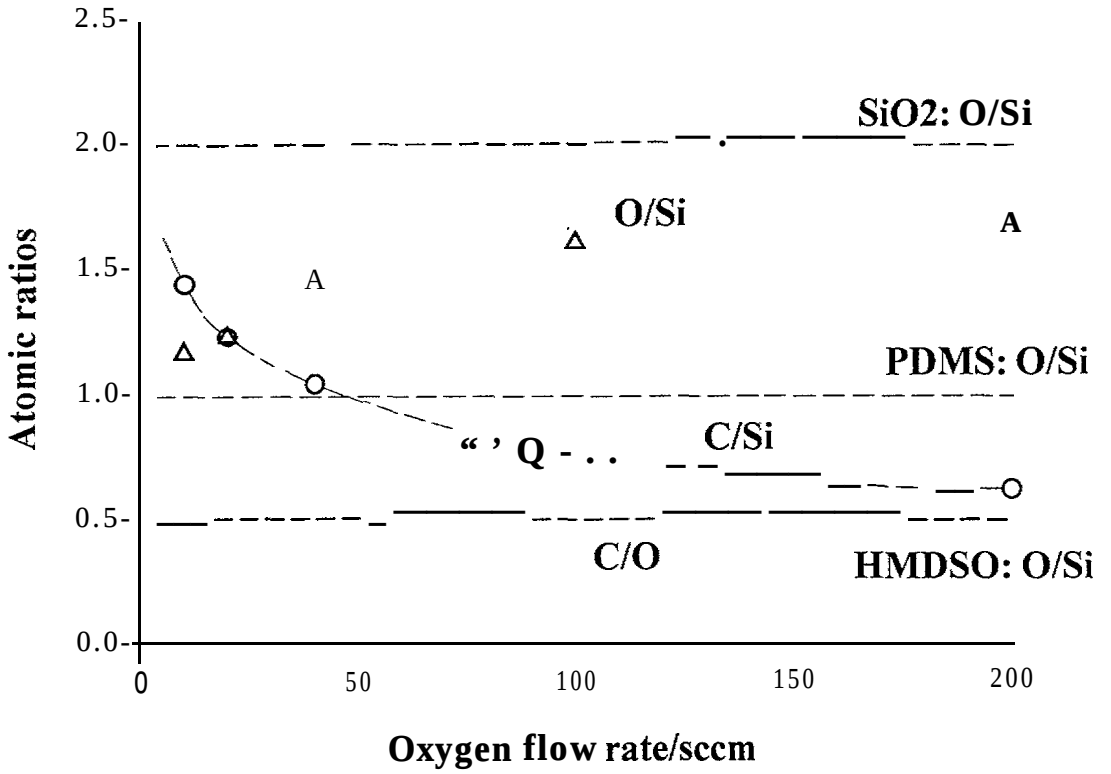

Figure. 5 Peak width (FWHM) ratios from HMDSO/O_2 plasma deposits -P=50 Pa, W=200 W, HMDSO flow rate =20 seem, film thickness=5 μm versus oxygen flow rate/sccm.

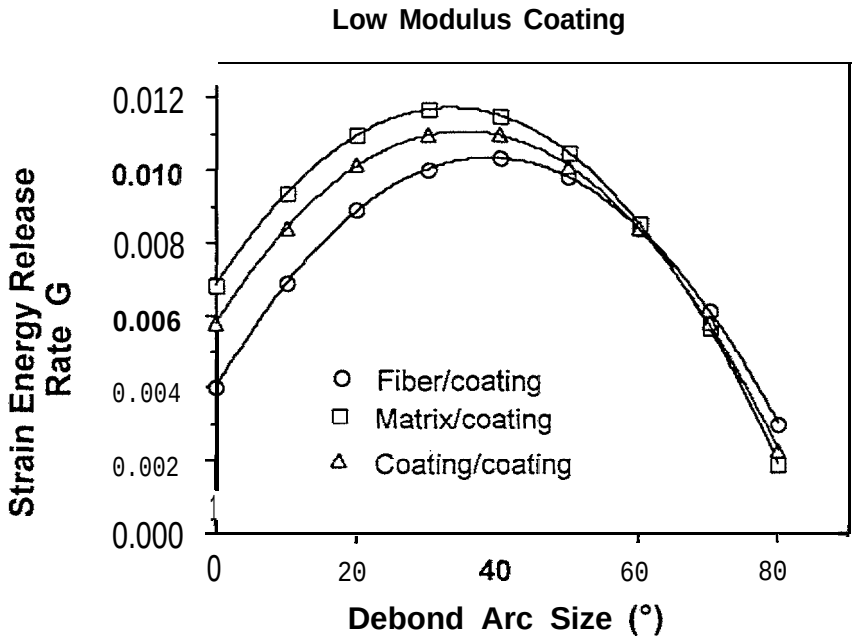

Fig. 12 Strain energy release rate for arc crack propagation along three different interfaces obtained from strain energy normalised against the strain energy of unit cell without crack. Results for low modulus coating.

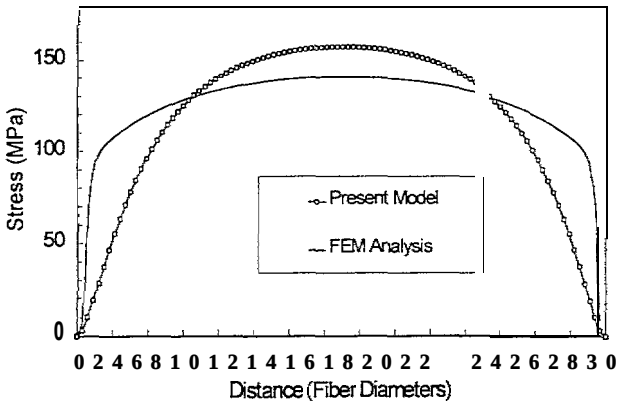

Fig. 13 The axial tensile stress in the fibre, σ_{zz}, as a function of distance (units: fibre diameter) along Z of Fig. 14 for a fragment of aspect ratio 30 in a three phase model. The stresses are plotted for the present model and FEM

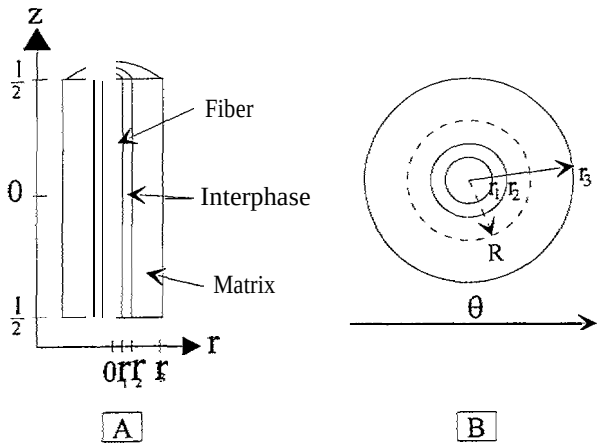

Fig, 14. A single fragment of a cracked fibre (tensile stress applied in z direction A: The three-cylinder model used in the axisymmetric stress analysis: a single fragment of length l showing the axial and radial co-ordinates. B: A cross-section of the three-cylinder model showing the fibre of radius r_1 and the interphase of radius r_2 and the matrix of radius r3

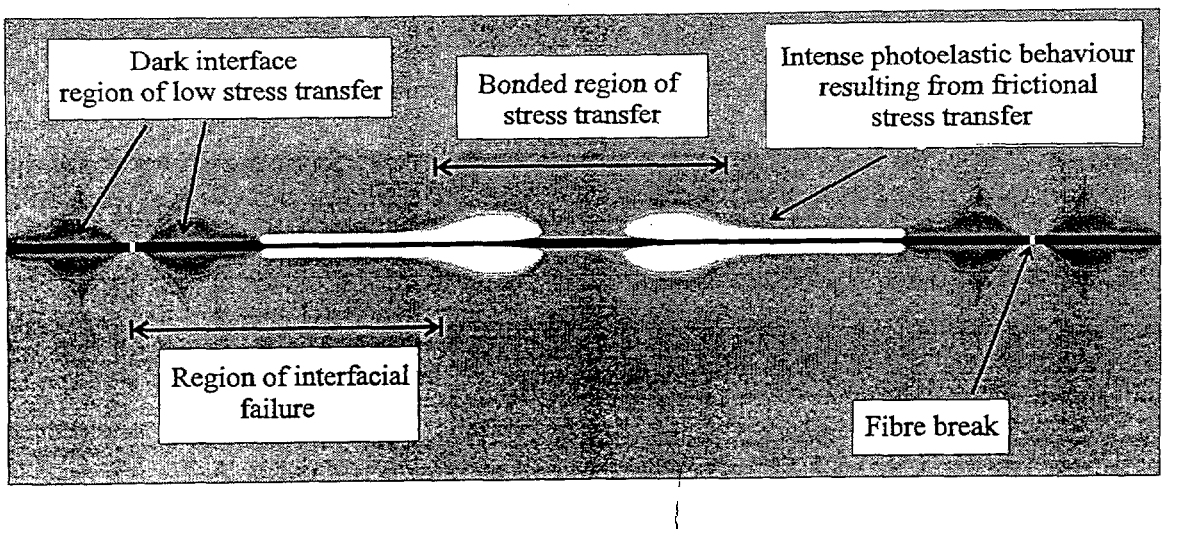

Figure 6 Schematic illustrate of the dark and light debonds in the SFFT.

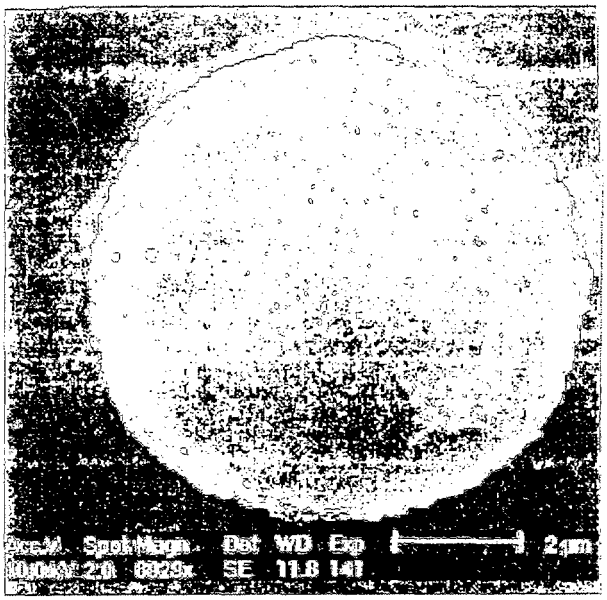

Fig. 7a Section of an untested, 02-pretreated fibre (600 W), 0.1 µm HMDSO/O_2 coating

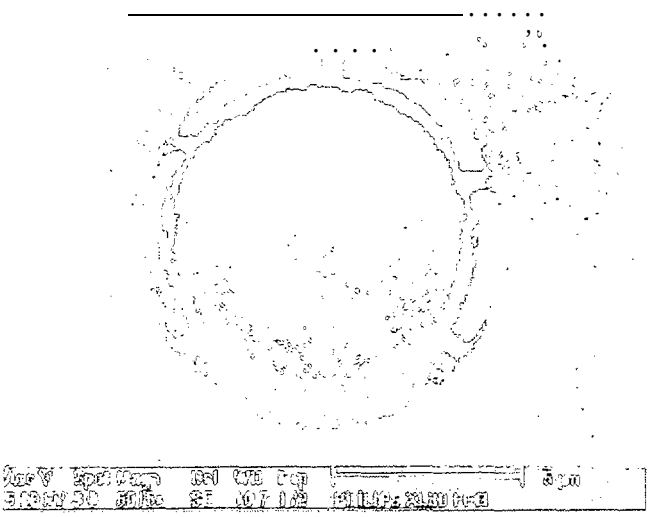

Fig. 7b Section of an untested, O_2-pretreated fibre (200 W), 0.5 µm HMDSO/O_2 coating

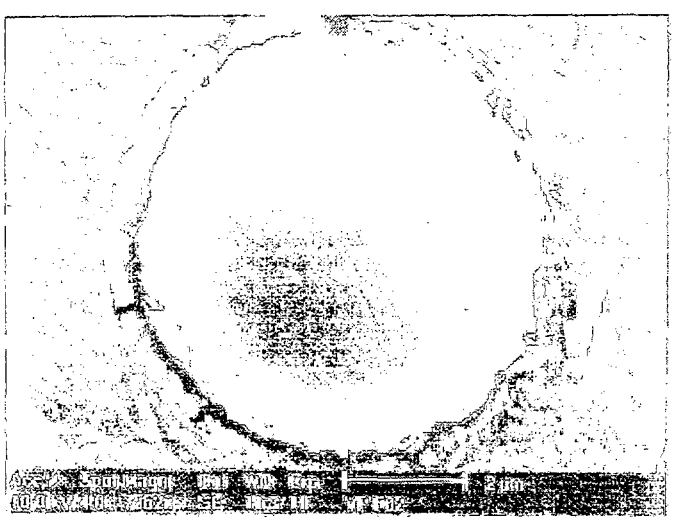

Fig. 7c Section of a tested, O_2-pretreated fibre (600W), 0.5 µm HMDSO/O_2 coating, position 1.

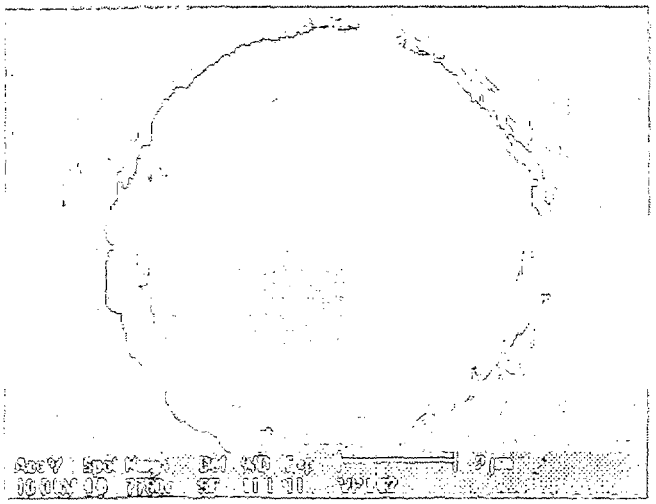

Fig. 7d Section of a tested, O_2-pretreated fibre (600W), 0.5 µm HMDSO/O_2 coating, position 2.

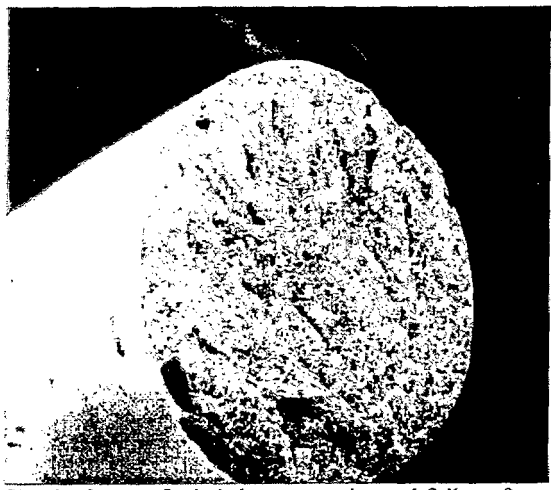

Fig. 8a SEM of a brittle composite rod failure for a 600W O_2 uncoated carbon fibres.

Fig. 8b : SEM of a tough failure for a composite rod formed with fibres with a 0.1 μm thick plasma coating and no pretreatment.

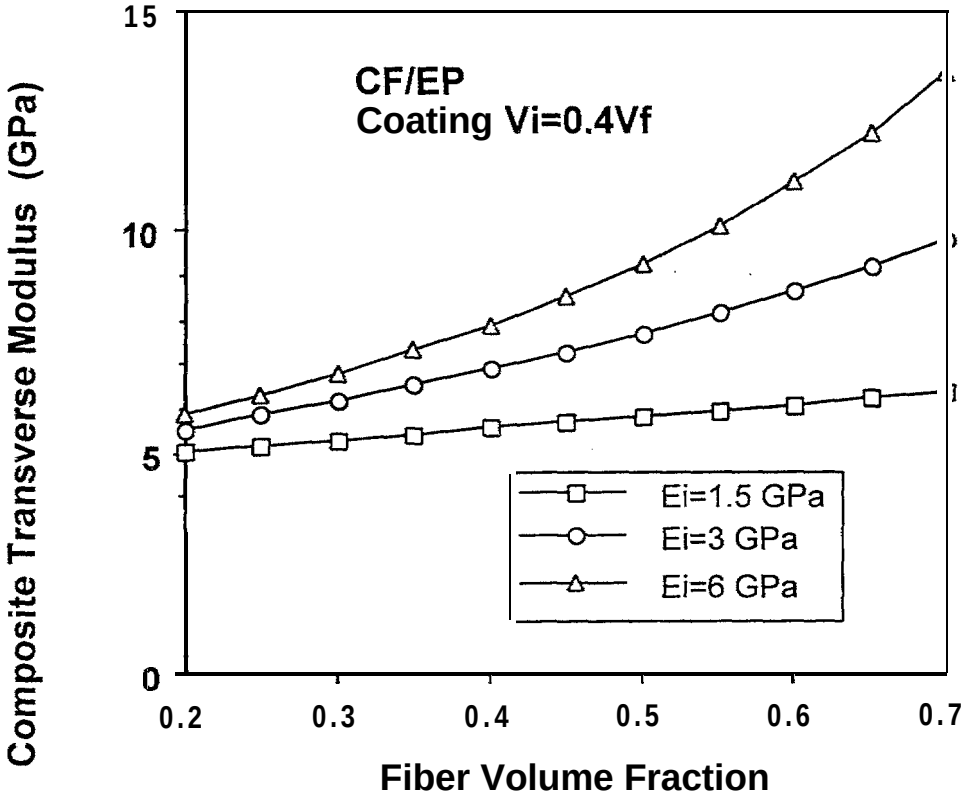

Fig.9 Transverse modulus of the coated fibre composite as a function of fibre volume fraction: effect of coating stiffness.

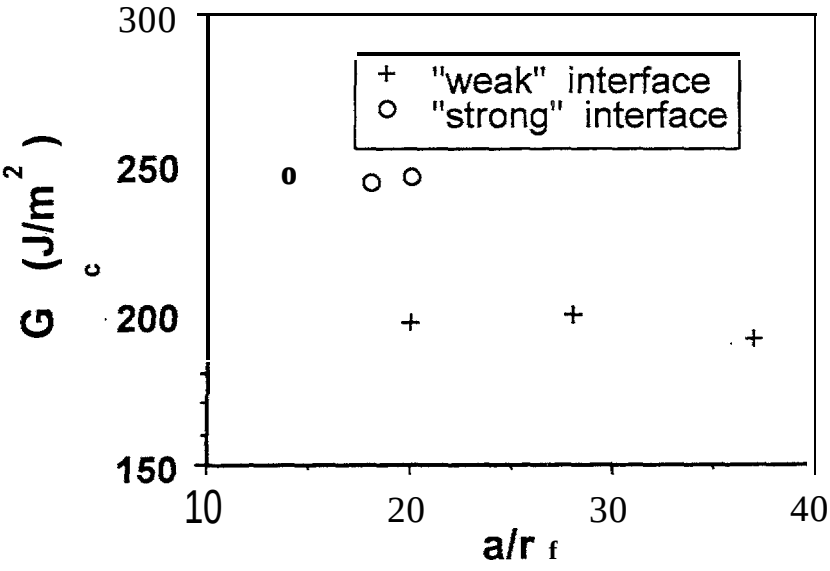

Figure 10. Critical strain energy release rate, G_C, at the fibre-matrix interface as *a* function of debond length for two single filament composites of differing interfacial strength.

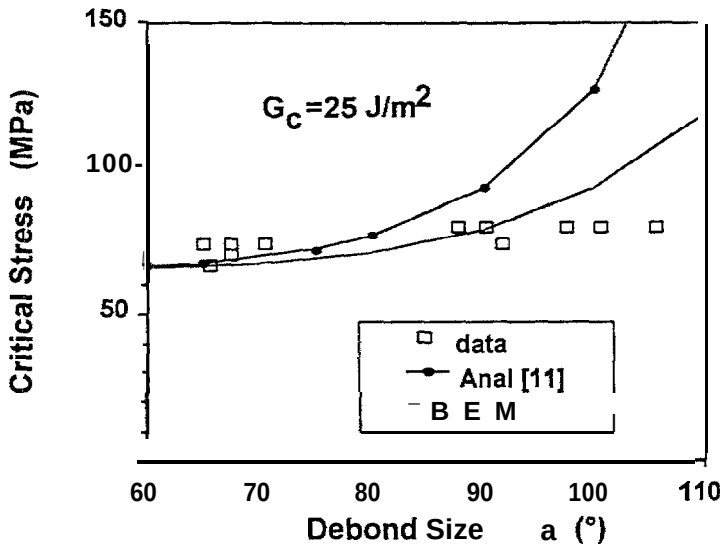

Fig. 11 Predictions and experimental data for debond growth . Critical stress for further growth as a function of debond arc size.